SEMI-BLIND DECONVOLUTION OF NEURAL IMPULSE RESPONSE IN fMRI USING A GIBBS SAMPLING METHOD

Salima Makni,[1] *Philippe Ciuciu,*[1] *Jérôme Idier,*[2] *and Jean-Baptiste Poline*[1]

[1]Service Hospitalier Frédéric Joliot (CEA) 4, Place du Général Leclerc, 91406 Orsay, France
[2]IRCCyN (CNRS), 1 rue de la Noë, BP 92101 44321 Nantes cedex 3, France
[1] name@shfj.cea.fr, [2] Jerome.Idier@irccyn.ec-nantes.fr

ABSTRACT

In functional Magnetic Resonance Imaging (fMRI), the Hemodynamic Response Function (HRF) represents the impulse response of the *neurovascular* system. Its identification is essential for a better understanding of cerebral activity since it provides a typical time course of the response to a stimulus in a given region of interest (ROI). In recent work [1], the authors have developed an HRF estimation method based on a single time course. Here, we propose an extension that takes the spatial homogeneity of the HRF into account. Our hypothesis based on biological results is that a ROI can be characterized by a single HRF but varying magnitude in space. Our goal is to estimate those magnitudes that could then be interpreted as a correlate of the neural response. We are thus faced with a *semi-blind deconvolution* inverse problem since the time arrivals of the neural response are known : they correspond to stimuli timing. To cope with this issue, we introduce specific prior information about the HRF and the neural response. Finally, we develop a MCMC approach to approximate the posterior mean estimates of unknown quantities. Simulation results show the improvement brought by our formulation compared to the approach developed in [1].

1. INTRODUCTION

Despite numerous investigations, the relation between the neuronal activity, in response to cognitive or behavioral tasks, and the Blood Oxygen Level-Dependent (BOLD) response [2], as measured with fMRI, is not completely understood [3]. A better quantification of the brain neuronal activity is still needed. The whole brain is usually modelled as a stationary, linear "black-box" system characterized by its impulse response, the HRF [4]. The HRF models information transfer from reception of the stimulus to measurement of the BOLD signal.

Neighbor voxels belonging to an homogeneous ROI of the brain demonstrate close shapes of the HRF but potentially different signal amplitudes. Taking this aspect into account should provide a more robust estimation of the HRF. The purpose of this paper is to estimate a single HRF shape in a given ROI and a scale factor for every voxel and stimulus type, that may better represent the neural response. This problem can therefore be identified as a *semi-blind deconvolution* inverse problem where the input sequence is the neural response and the filter is the HRF given the biological hypotheses. Since the stimuli timing is known, structural knowledge on the input sequence is available to constrain HRF estimation, leading to a partially blind problem.

To get a robust estimation of all parameters, we develop a Bayesian approach using physiological prior information. The HRF is modelled as a smooth function. The stimulus-dependent neural response levels are assumed to be independent across voxels as well as across stimulus types or conditions. The hyperparameters that govern Gaussian prior distributions as well as noise variances (one per voxel) have to be estimated in an appropriate way. To address this issue, we derive the posterior distribution and reliable estimates of both the hyperparameters and of the parameters of interest. For simplicity reasons, we compute posterior mean estimates from samples of the unknown quantities, generated using a Gibbs sampler algorithm. This approach is tested on realistic simulated data. Compared to [1], a significant gain is achieved in terms of accuracy and computational cost. It also corresponds to a simpler model since a single HRF for each ROI and all conditions is estimated instead of one per voxel and condition as in [1].

2. PROBLEM FORMULATION

2.1. Voxel-based model

In event-related fMRI with synchronous inter-stimulus interval, the BOLD time course $(y_{t_n})_{1\leq n\leq N}$ is measured in any voxel of the brain at times $(t_n = nTR)_{1\leq n\leq N}$, TR being the Repetition Time, while stimuli occur with a fixed-delayed impulse signal $(x_{t_n})_{1\leq n\leq N}$. The sampling period is then TR when the stimuli occur at times of acquisition.

In *asynchronous* experiments, the presented stimuli occur at any time during scanning. In such cases, the data and

the trials are combined on a finer temporal grid defined by a sampling period $\Delta t <$ TR. The occurrences of the stimuli $(x_t)_{t \geqslant t_1}$ match time points on this grid such that two stimuli never occur at the same time. Assuming the neurovascular system linear and time-invariant, the fMRI data are related to the stimulus sequence as follows :

$$y_{t_n} = \sum_{k=0}^{K} h_{k\Delta t} x_{t_n - k\Delta t} + b_{t_n}, \qquad \forall n \in \{1, \ldots, N\} \quad (1)$$

where $\boldsymbol{x}_{t_n} = [x_{t_n}, x_{t_n - \Delta t}, \ldots, x_{t_n - K\Delta t}]^{\mathrm{t}}$ and $\boldsymbol{h} = [h_0, h_{\Delta t}, \ldots, h_{K\Delta t}]^{\mathrm{t}}$. b_{t_n} is the nth sample of a zero-mean Gaussian AR(1) noise process $\boldsymbol{b}$ independent of $\boldsymbol{h}$. Let ρ be the AR coefficient, $\boldsymbol{b}$ is the ouput of the linear system defined by $T(z) = (1 - \rho z^{-1})^{-1}$, whose input sequence $\boldsymbol{\epsilon}$ is $\mathcal{N}(\boldsymbol{0}, \sigma_\epsilon^2 \boldsymbol{I})$-distributed. This noise model is appropriate to account for temporal correlation of fMRI data due to physiological artifacts. Let $\boldsymbol{X} = [\boldsymbol{x}_{t_1}, \ldots, \boldsymbol{x}_{t_N}]^{\mathrm{t}}$, (1) can be written in a matrix equation :

$$\boldsymbol{y} = \boldsymbol{X}\boldsymbol{h} + \boldsymbol{b}, \qquad \text{with } \boldsymbol{b} \sim \mathcal{N}(\boldsymbol{0}, \sigma_b^2 \boldsymbol{\Gamma}), \quad (2)$$

where $\boldsymbol{\Gamma}$ is the covariance matrix of an AR(1) process. The stationarity of the system is ensured by the following condition : $(1 - \rho^2)\sigma_b^2 = \sigma_\epsilon^2$.

2.2. Region-based model

In functional neuroimaging, we are primarily interested in detecting functionally homogeneous clusters of voxels involved in the same way in a given cognitive task. Once such an homogeneous ROI has been found out, we search for the *canonical* time response of this ROI. There exist several concurrent approaches to perform this analysis. The most widespread consists in computing a spatial summary of the data (*e.g.,* the mean) over the ROI to get a single time course before estimating the corresponding HRF [5]. Here, we propose a ROI-based HRF estimate *without spatial averaging of the data*. To this end, we introduce a generalization of (2) that accounts for a voxel-dependent signal and noise levels but assumes a single HRF shape over the region. Let $\mathcal{R} = \{V_1, \ldots, V_J\}$ be the ROI with J voxels and $\boldsymbol{y}_j$ the fMRI data of voxel V_j, model (2) becomes :

$$\boldsymbol{y}_j = a_j \boldsymbol{X}\boldsymbol{h} + \boldsymbol{b}_j, \qquad \forall j \in \{1, \ldots, J\}. \quad (3)$$

where a_j stands for the neural response level in V_j. Note that the experiment consists of several occurrences of the same stimulus. Since we assume a *time-invariant* neurovascular system, parameter a_j is constant in time. As shown in [6], this assumption is a tenable and useful approximation.

Several noise models can be considered for $\mathcal{R}$ depending on its spatial properties. The simplest is an independent and identically distributed (i.i.d.) AR(1) model, specified by the above mentioned parameters $(\rho, \sigma_\epsilon^2)$. Nonetheless, due to partial volume effect[1] in fMRI data, the noise level may strongly vary from one voxel to another. This requires a slightly more complicated model, in which a specific noise variance $\sigma_{b_j}^2$ or equivalenty $\sigma_{\epsilon_j}^2$ is attributed to each voxel V_j. Vector $\boldsymbol{\sigma}_{\boldsymbol{\epsilon}}^2 = \left[\sigma_{\epsilon_1}^2, \ldots, \sigma_{\epsilon_J}^2\right]^{\mathrm{t}}$ is unknown and should be estimated as well. For computational reasons, we do not consider spatially non-stationary AR processes, even if they may better reflect the gray-white matter interface of the brain [7].

2.3. Multicondition extension

Actual fMRI experiments consist of several stimulus types or conditions (visual, auditory,..). We further extend model (3) to estimate neural impulse levels that vary with the stimulus type. Let $\left(\boldsymbol{X}^{(m)}\right)_{1 \leqslant m \leqslant M}$ be the different stimulus-dependent matrices, corresponding to the previous $\boldsymbol{X}$ matrix but implementing a condition specific model, and then suppose that the responses to stimulus m in V_j, add in a *linear* way, then the generalization of (3) is given by

$$\boldsymbol{y}_j = \sum_{m=1}^{M} a_j^m \boldsymbol{X}^{(m)} \boldsymbol{h} + \boldsymbol{b}_j, \qquad \forall j \in \{1, \ldots, J\}.$$

Note that $\boldsymbol{h}$ is not stimulus-dependent. To estimate the HRF and the neural response levels $\boldsymbol{A} = (a_j^m)_{1 \leqslant j \leqslant J}^{1 \leqslant m \leqslant M}$, we first need to take this model into account through the definition of the likelihood function. If the fMRI time series $\boldsymbol{Y} = [\boldsymbol{y}_1, \ldots, \boldsymbol{y}_J]$ are supposed to be statistically independent, the likelihood $p(\boldsymbol{Y}|\boldsymbol{h}, \boldsymbol{A})$ reads :

$$p(\boldsymbol{Y} \mid \boldsymbol{h}, \boldsymbol{A}, \boldsymbol{\sigma}_{\boldsymbol{\epsilon}}^2) = \prod_{j=1}^{J} p(\boldsymbol{y}_j \mid \boldsymbol{h}, \boldsymbol{A}, \boldsymbol{\sigma}_j^2) = \prod_{j=1}^{J} (2\pi\sigma_{b_j}^2)^{-N/2}$$

$$|\boldsymbol{\Gamma}|^{-1/2} \exp\Big(-\sum_{j=1}^{J} ||\boldsymbol{y}_j - \sum_{m=1}^{M} a_j^m \boldsymbol{X}^{(m)} \boldsymbol{h})||_{\boldsymbol{\Gamma}^{-1}}^2 / 2\sigma_{b_j}^2\Big) \quad (4)$$

$$\propto \prod_{j=1}^{J} \sigma_{\epsilon_j}^{-N} |\boldsymbol{\Sigma}|^{1/2} \exp\Big(-\frac{\sum_{j=1}^{J} ||\boldsymbol{y}_j - \sum_{m=1}^{M} a_j^m \boldsymbol{X}^{(m)} \boldsymbol{h})||_{\boldsymbol{\Sigma}}^2}{2\sigma_{\epsilon_j}^2}\Big)$$

where the inverse of the autocorrelation matrix $\boldsymbol{\Gamma}$ is [8] :

$$\boldsymbol{\Sigma} \triangleq \boldsymbol{\Gamma}^{-1} = \begin{bmatrix} 1 & -\rho & 0 & \cdots & \cdots & 0 \\ -\rho & 1+\rho^2 & -\rho & 0 & \ddots & \vdots \\ 0 & \ddots & \ddots & \ddots & \ddots & \vdots \\ \vdots & \ddots & \ddots & \ddots & \ddots & 0 \\ \vdots & \ddots & 0 & -\rho & 1+\rho^2 & -\rho \\ 0 & \cdots & \cdots & 0 & -\rho & 1 \end{bmatrix}.$$

Maximum likelihood (ML) estimation of $(\boldsymbol{h}, \boldsymbol{A})$ is a bilinear inverse problem since $p(\boldsymbol{Y} \mid \boldsymbol{h}, \boldsymbol{A}, \boldsymbol{\sigma}_{\boldsymbol{\epsilon}}^2)$ is linear with

[1] Gray and white matter are mixed in variable proportion in different voxels.

respect to $\boldsymbol{h}$ when $\boldsymbol{A}$ is fixed and *vice-versa*. In addition, this problem is ill-posed since the ML solution $(\boldsymbol{h}^*, \boldsymbol{A}^*)$ is not unique. For instance, any couple $(\boldsymbol{h}^*/C, \boldsymbol{A}^* \star C)$ defines a solution in the ML sense. By contrast, structural prior information is available both on $\boldsymbol{h}$ and $\boldsymbol{A}$. To solve this ill-posed problem, we develop in the following a model within the Bayesian framework.

3. A SEMI-BLIND DECONVOLUTION APPROACH

3.1. Prior information

The HRF. As physiologically advocated in [3], the canonical BOLD response to a stimulus *i.e.,* the HRF, can be characterized by the following features [1] : *(i)* its variations are smooth ; *(ii)* the HRF is causal and returns to a baseline after about 25 sec : its amplitude is close to zero at the first and end time points. To fullfil conditions *(i)-(ii)*, we use a Gaussian distribution $p(\boldsymbol{h}; \sigma^2_{\boldsymbol{h}}, \boldsymbol{R}) = \mathcal{N}(0, \sigma^2_{\boldsymbol{h}}\boldsymbol{R})$ where $\boldsymbol{R} = (\boldsymbol{D}_2^{\mathrm{t}}\boldsymbol{D}_2)^{-1}$ and $\boldsymbol{D}_2$ is the truncated second-order finite difference matrix to account for $h_0 = h_{K\Delta t} = 0$.

The "neural" responses. It is reasonable to assume that different types of stimulus induce statistically independent neural responses [3]. Thus we choose $p(\boldsymbol{A};\boldsymbol{\theta}_{\boldsymbol{A}}) = \prod p(\boldsymbol{a}^m, \boldsymbol{\theta}_m)$ with $\boldsymbol{a}^m = [a_1^m, \ldots, a_J^m]$. For condition m, the neural response level is assumed to be $\mathcal{N}(\mu^m, \sigma^2_m)$-distributed. Moreover, vector $\boldsymbol{a}^m$ is a set of independent realizations since we do not model any spatial correlation between the response levels of neighbor voxels.

The hyperparameters. The complete set of hyperparameters to be estimated is denoted $\boldsymbol{\Theta} = [\boldsymbol{\sigma}_{\boldsymbol{\epsilon}}, \boldsymbol{\theta}_{\boldsymbol{A}}]$. It consists of voxels noise variances on one hand, and location and scaling parameters $\boldsymbol{\theta}_m = (\mu^m, \sigma^2_m)$ of $p(\boldsymbol{a}^m, \boldsymbol{\theta}_m)$ on the other hand. For $\boldsymbol{\theta}_m$, we resort to non informative priors such as *Jeffreys* pdf for σ^2_m. Other hyperparameter $(\sigma^2_{\boldsymbol{h}}, \rho)$ are set empirically. We have chosen $\sigma^2_{\boldsymbol{h}} = 1$ to solve for the scale ambiguity encountered in blind deconvolution problems [9]. For simplicity reasons, the AR coefficient is set to $\rho = 0.9$ to account low-frequency drift in an appropriate way.

3.2. Posterior distribution

The posterior pdf of $(\boldsymbol{h}, \boldsymbol{A}, \boldsymbol{\Theta})$ reads :

$$p(\boldsymbol{h}, \boldsymbol{A}, \boldsymbol{\Theta}|\boldsymbol{Y}) \propto p(\boldsymbol{Y}|\boldsymbol{h}, \boldsymbol{A}, \boldsymbol{\sigma}^2_{\boldsymbol{\epsilon}}) p(\boldsymbol{h}) p(\boldsymbol{A}|\boldsymbol{\theta}_{\boldsymbol{A}}) p(\boldsymbol{\theta}_{\boldsymbol{A}}) p(\boldsymbol{\sigma}^2_{\boldsymbol{\epsilon}}).$$

Due to the bilinearity aspect of $p(\boldsymbol{h}, \boldsymbol{A}, \boldsymbol{\Theta} \,|\, \boldsymbol{Y})$, we do not choose the Maximum *A Posteriori* estimate of $(\boldsymbol{h}, \boldsymbol{A})$. Indeed, its computation requires stochastic optimization since many local maxima may exist in the energy landscape of $p(\boldsymbol{h}, \boldsymbol{A}, \boldsymbol{\Theta}|\boldsymbol{Y})$. Moreover, MAP estimation does not provide any response to hyperparameter tuning. We rather propose a Gibbs sampling algorithm, which has shown to be relevant in the context of blind deconvolution problems [9]. We generate realizations of $p(\boldsymbol{h}, \boldsymbol{A}, \boldsymbol{\Theta} \,|\, \boldsymbol{Y})$ using sequential sampling from the conditional posterior pdfs. To do that, we account for the bilinearity and draw samples from the Gaussian distributions $p(\boldsymbol{h}|\boldsymbol{Y}, \boldsymbol{A}, \boldsymbol{\Theta})$ and $p(\boldsymbol{A}|\boldsymbol{Y}, \boldsymbol{h}, \boldsymbol{\Theta})$. Finally, for $(\boldsymbol{h},\boldsymbol{A})$ we compute an estimate of the *a posteriori* expectation (EAP), which is different from the MAP since the posterior pdf is not Gaussian. For hyperparameters $\boldsymbol{\Theta}$, we also resort to posterior mean estimates.

3.3. Computational details

The conditional posterior distribution of $\boldsymbol{h}$, $\boldsymbol{A}$ and $\boldsymbol{\sigma}^2_{\boldsymbol{\epsilon}}$ is simply proportionnal to the product of the likelihood (4) and their relative priors $p(\boldsymbol{h})$, $p(\boldsymbol{A}; \boldsymbol{\theta}_{\boldsymbol{A}})$ and $p(\boldsymbol{\sigma}^2_{\boldsymbol{\epsilon}}) = \prod_j p(\sigma^2_{\epsilon_j})$ $= \prod_j \sigma^{-2}_{\epsilon_j}$, in accordance with Bayes rule. We get

$$\begin{aligned}
p(\boldsymbol{h}|\boldsymbol{Y}, \boldsymbol{A}, \boldsymbol{\sigma}^2_{\boldsymbol{\epsilon}}) &\sim \mathcal{N}(m_{\boldsymbol{h}}, \boldsymbol{\Sigma}_{\boldsymbol{h}}) \\
\boldsymbol{\Sigma}_{\boldsymbol{h}} &= (\boldsymbol{R}^{-1} + \sum_j ||\sum_m a_j^m \boldsymbol{X}^{(m)}||^2_{\boldsymbol{\Sigma}}/\sigma^2_{\epsilon_j})^{-1} \qquad (5) \\
m_{\boldsymbol{h}} &= \boldsymbol{\Sigma}_{\boldsymbol{h}} \sum_j (\sum_m a_j^m \boldsymbol{X}^{(m)})^{\mathrm{t}} \boldsymbol{\Sigma} \boldsymbol{y}_j/\sigma^2_{\epsilon_j},
\end{aligned}$$

$$p(\boldsymbol{A}|\boldsymbol{Y}, \boldsymbol{h}, \boldsymbol{\sigma}^2_{\boldsymbol{\epsilon}}) = \prod_j \Big[p(\boldsymbol{a}_j \,|\, \boldsymbol{y}_j, \boldsymbol{h}, \sigma^2_{\epsilon_j}) \sim \mathcal{N}(m_{\boldsymbol{a}_j}, \boldsymbol{\Sigma}_{\boldsymbol{a}_j}) \Big] \quad (6)$$

$$\begin{aligned}
\boldsymbol{\Sigma}^{-1}_{\boldsymbol{a}_j} &= \mathbb{X}^{\mathrm{t}} \boldsymbol{\Sigma} \mathbb{X}/\sigma^2_{\epsilon_j} + \mathrm{diag}\left[\sigma_1^{-2}, \cdots, \sigma_M^{-2}\right] \\
m_{\boldsymbol{a}_j} &= \boldsymbol{\Sigma}_{\boldsymbol{a}_j} \left(\mathbb{X}^{\mathrm{t}} \boldsymbol{\Sigma} \boldsymbol{y}_j/\sigma^2_{\epsilon_j} + \left[\mu^1/\sigma^2_1, \cdots, \mu^M/\sigma^2_M\right]^{\mathrm{t}} \right),
\end{aligned}$$

$$p(\sigma^2_{\epsilon_j} | \boldsymbol{y}_j, \boldsymbol{h}, \boldsymbol{a}_j) \sim \mathcal{IG}(\frac{N}{2}, ||\boldsymbol{y}_j - \sum_m a_j^m \boldsymbol{X}^{(m)} \boldsymbol{h})||^2_{\boldsymbol{\Sigma}}/2), \quad (7)$$

where $\mathbb{X} = [\boldsymbol{X}^{(1)}\boldsymbol{h} \,|\, \cdots \,|\, \boldsymbol{X}^{(M)}\boldsymbol{h}]$. To estimate μ^m and σ^2_m, we use the following proposition (*cf.* [10, p. 187]).

Proposition 1 *If vector $\boldsymbol{a}^m$ is a set of $\mathcal{N}(\mu^m, \sigma^2_m)$-distributed i.i.d. observations, the posterior distribution of (μ^m, σ^2_m) associated with the prior distribution $\widetilde{\pi}(\mu^m, \sigma_m) = \sigma_m^{-1}$ is*

$$\begin{aligned}
\mu^m \,|\, \sigma^2_m, \overline{\boldsymbol{a}}^m, s^2 &\sim \mathcal{N}(\overline{\boldsymbol{a}}^m, \sigma^2_m/J) \qquad (8) \\
\sigma^2_m \,|\, \overline{\boldsymbol{a}}^m, s^2 &\sim \mathcal{IG}((J-1)/2, s^2/2) \qquad (9)
\end{aligned}$$

where $\overline{\boldsymbol{a}}^m = \sum_{j=1}^J a_j^m/J$ and $s^2 = \sum_{j=1}^J (a_j^m - \overline{\boldsymbol{a}}^m)^2$ are sufficient statistics.

We summarize the Gibbs sampling algorithm as follows :

(1) Initialization : choose $\boldsymbol{A}^0$, $(\boldsymbol{\sigma}^2_{\boldsymbol{\epsilon}})^0$, $\boldsymbol{\theta}^0_{\boldsymbol{A}}$.

(2) Iteration k : draw samples $\boldsymbol{h}^k$, $\boldsymbol{A}^k$, $(\boldsymbol{\sigma}^2_{\boldsymbol{\epsilon}})^k$, $\boldsymbol{\theta}^k_{\boldsymbol{A}}$ from the conditional posterior distributions (5)- (9).

(3) Iterate until maximum iteration number K_0 is achieved.

Finally, we compute posterior mean estimates using the following approximation :

$$\widehat{\theta}^{EAP} = \sum_{k=I}^{K_0} \theta^k/(K_0 - I + 1), \ \forall \theta \in \left\{\boldsymbol{h}, \boldsymbol{A}, \boldsymbol{\sigma}^2_{\epsilon}, \boldsymbol{\mu}_{\boldsymbol{a}}, \boldsymbol{\sigma}^2_{\boldsymbol{a}}\right\}$$

where I defines the discarded burn-in period[2].

[2]The corresponding samples are not drawn from the target posterior distribution.

4. SIMULATION RESULTS

We tested our method using realistic synthetic data and compared it to previous work [1]. We considered a ROI composed of $J = 10$ voxels. We simulated a random inter mixed sequence of indices coding for $M = 2$ different stimuli. Two sets of trials (for $m = 1$ and $m = 2$) were generated, each of them corresponding to a specific stimulus. These binary time series were multiplied by a stimulus-dependent scale factor. For $m = 1$, the stimulus was not homogeneous in space to assess the robustness of our approach. We used scale factors (a_j^1) divided into two spatially homogeneous subsets : magnitudes $a^1_{1,\dots,7}$ and $a^1_{8,\dots,10}$ were drawn from $\mathcal{N}(\mu^1 = 2, \sigma_1^2 = 0.1)$ and $\mathcal{N}(\widetilde{\mu}^1 = 8, \sigma_1^2 = 0.1)$, respectively. For $m = 2$, the stimulus was homogeneous in space and followed a $\mathcal{N}(\mu_1^2 = 10, \sigma_2^2 = 0.1)$ distribution. Both time series were then convolved with the so-called canonical HRF $\boldsymbol{h}_c$ (see Fig. 1(c)) used in the SPM99 software[3]. In all voxels, the number of data is $N = 100$ in all cases. A correlated Gaussian noise $(\sigma_\epsilon^2, \rho) = (0.3, 0.9)$ has been added to the data. The corresponding signal-to-noise ratio is similar to those encountered in real fMRI data.

Fig 1(a)-(b) show the estimated neural response levels for both conditions in all voxels. These estimates accurately match the true values despite the spatial inhomogeneity introduced for the first condition. The HRF estimate plotted in Fig 1(c) is very close to $\boldsymbol{h}_c$ that appear on the same graph in dotted line. The stimulus-dependent HRF estimates depicted in Fig. 1(d) have been computed from the spatial average of the data over the ROI using the previous approach [1]. These estimates are very similar to the scaled true HRFs $\bar{a}^1 \star \boldsymbol{h}_c$ and $\bar{a}^2 \star \boldsymbol{h}_c$, respectively, with $\bar{a}^m = \sum_j a_j^m / J$. We therefore show that we can retrieve spatially varying response magnitude while this cannot be easily achived with method [1] since a voxel-based approach would be time-consuming and too noisy. Spatial selectivity is of primary interest in fMRI since the ROI is often not homogeneous for some stimulus type. As illustrated, our approach provides an efficient and appropriate response to take the spatial variation of the neural response into account.

5. CONCLUSION

We have proposed an original method for semi-blind deconvolution of impulse neural response in functional neuroimaging. This method extends previous work [1] to deal with regional HRF estimation in a efficient way while modeling the spatial variability of the neural response for each type of stimulus. We have validated this approach on realistic synthetic data. Future work will investigate its use on real fMRI data.

[3] www.fil.ion.ucl.ac.uk/spm/spm99.html

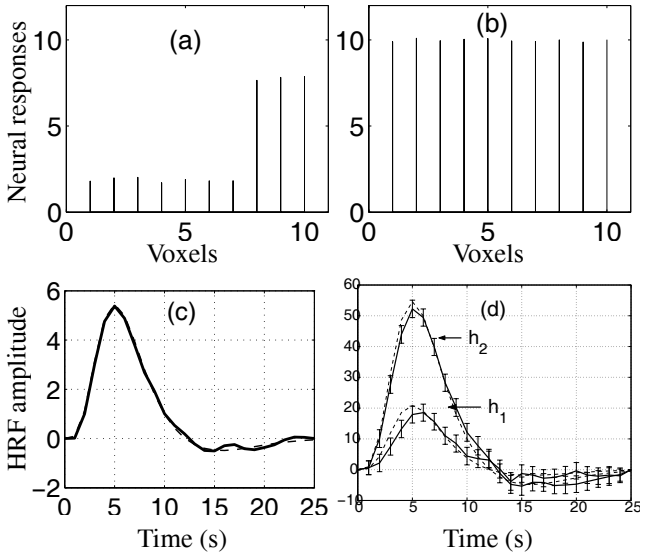

Fig. 1. (a)-(b) estimates of neural response levels a_j^1 and a_j^2 ; (c), true HRF $\boldsymbol{h}_c$ (- -), regional HRF estimate (–) ; (d) true HRFs (- -) : $\boldsymbol{h}_m = \bar{a}_m \star \boldsymbol{h}_c,\ m = 1, 2$ and voxel-based HRF estimates (–) : $\widehat{\boldsymbol{h}}_m = \widehat{\bar{a}}_m \star \boldsymbol{h}_c$.

6. REFERENCES

[1] P. Ciuciu, J.-B. Poline, G. Marrelec, J. Idier, C. Pallier, and H. Benali, "Unsupervised robust non-parametric estimation of the hemodynamic response function for any fMRI experiment," *IEEE Trans. Medical Imaging*, vol. 22, no. 10, pp. 1235–1251, Oct. 2003.

[2] S. Ogawa, T. Lee, A. Kay, and D. Tank, "Brain magnetic resonance imaging with contrast dependent on blood oxygenation," *PNAS USA*, vol. 87, no. 24, pp. 9868–9872, 1990.

[3] R. Buxton and L. Frank, "A model for the coupling between cerebral blood flow and oxygen metabolism during neural stimulation," *J. Cereb. Blood Flow Metab.*, vol. 17, no. 1, pp. 64–72, 1997.

[4] R. L. Buckner, and al., "Functional-anatomic correlates of object priming in humans revealed by rapid presentation event-related fMRI," *Neuron*, vol. 20, pp. 285–296, 1998.

[5] M. Brett, J.-L. Anton, R. Valabregue, and J.-B. Poline, "Region of interest analysis using an SPM toolbox," in *Proc. 8th HBM*, Sendai, Japan, June 2002.

[6] G. H. Glover, "Deconvolution of impulse response in event-related BOLD fMRI,"*Neuroimage*, vol.9, pp.416–429, 1999.

[7] M. Woolrich and S. Smith, "Spatio-temporal noise model selection in fMRI," in *Proc. 8th HBM*, Sendai, Japan, June 2002.

[8] S. M. Kay, *Modern Spectral Estimation*, Prentice-Hall, Englewood Cliffs, NJ, 1988.

[9] Q. Cheng, R. Chen, and T.-H. Li, "Simultaneous wavelet estimation and deconvolution of reflection seismic signals," *IEEE Trans. Geosci. Remote Sensing*, vol. 34, pp. 377–384, 1996.

[10] C. P. Robert, *The Bayesian Choice. Second Edition*, Springer Texts in Statistics. Springer Verlag, New York, NY, 2001.